A.V. Arkhipov, M.V. Mishin, G.G. Sominski
St. Petersburg Polytechnic University

ANALYZER OF HIGH-LOAD ELECTRON BEAMS WITH RESOLUTION IN TWO ENERGY COMPONENTS, SPACE AND TIME

The new apparatus is developed for experimental determination of electron energy and spatial distributions in dense medium-energy long-pulsed magnetically confined beams − typically, 10 A/cm², 60 keV, 100 μs, 0.1 T. To provide most detailed and unambiguous information, direct electrostatic cut-off method is used for electron energy analysis. In combination with variation of the magnetic field in the analysis area, this method allows to determine both (axial and transverse) components of electron energy. Test experiments confirmed ~1% energy resolution being predicted from calculations, accounting for electrode shapes, space-charge effects and non-adiabatic energy transfer effects in varied magnetic field. Space and time resolution of the apparatus are determined by the input aperture size (~1 mm) and cut-off electric field pulse-length (~5-10μs) respectively.

ELECTRON BEAM, ELECTRON ENERGY DISTRIBUTION, RETARDING FIELD ANALYZER, ELECTRON-OPTICAL SYSTEM.

1. Introduction

Diagnostics of dense long-pulse electron beams, being necessary for their successful utilization, represents a serious problem because of high energy density carried by the beam and transferred to any irradiated surface. This may (and often does) entail development of rather complicated phenomena, affecting the measurements, such as generation of plasmas and secondary particle flows, both in the beam facility and in the diagnostic apparatus. Thus, minimization of such parasitic effects must be among the primary purposes for diagnostic systems' design.

In our case, the objective of further improvement of material processing techniques at GESA-series material-treatment electron beam facilities [1] required accurate measurement of electron energy distributions at the target, with resolution in position over the beam cross-section and in time within the facility current pulse. Typical GESA electron beam parameters are the following: an electron acceleration voltage $U_0 = 60 − 400$ kV, a beam current at the target is of $50 − 500$ A corresponding to a current density up to 10 A/cm², a guiding magnetic field at the target $B_0 = 0.02 − 0.10$ T, an operation in single pulses with a duration of $10 − 100$ μs. The new "Soffron60" electron beam analyzer was specially designed for operation at these conditions, near the lower limit of U_0. It was intended to supplement the "wells" measurement technique [2], installed earlier and providing very operative though rather generalized data on electron energy distribution parameters − in most cases, only the mean pitch angle of electron trajectories.

2. General scheme and electrode configuration

In the new Soffron60 analyzer, axial (parallel to the guiding magnetic field) component of electron energy is measured with electric cut-off method characterized by high resolution and reliability and allowing data cross-checking. Electron-optical scheme of the apparatus is presented in Fig.1. A partial beam is cut at the target of the facility with 1 mm input aperture and directed to the probe (Ref. No 7 in Fig. 1) inside a system of retarding electrodes. To these electrodes, a pulse of negative potential $−U_{ret}(t)$ is applied. Electrons reach the probe only if their axial energy eU_0 (in eV) exceeds absolute value of varied retarding potential. Comparison of retarding potential and a probe current I_{pass} pulses gives sufficient information for reconstruction of axial energy distribution in the partial beam, if its current at the input is constant during the measurement. Otherwise,
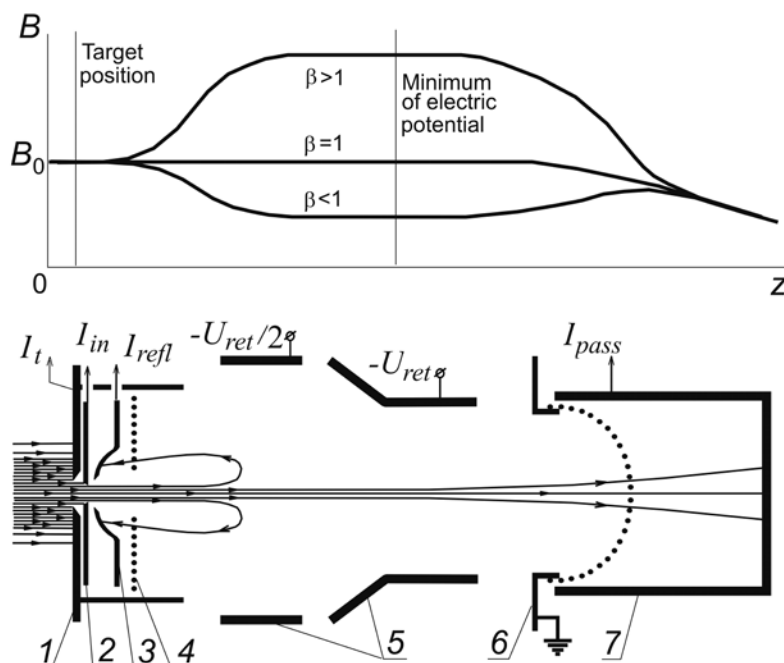
Fig. 1. Electron-optical scheme of Soffron60 analyzer: a target with input aperture (*1*), input current probe (*2*), collector of reflected electrons (*3*); mesh shields (*4, 6*), retarding field electrodes (*5*), passing current probe (*7*).
The plot at the top represents possible distributions of magnetic field in the analyzer for three values of magnetization ratio β. I_{in}, I_{refl}, I_{pass} are input, reflected and passing probe currents; $-U_{ret}$ is the negative potential applied to retarding field electrodes

the input current I_{in} and/or current of electrons reflected from the negative potential I_{refl} are to be determined also. For this purpose, special two additional current probes (Refs. No *2* and *3* in Fig. 1) are introduced in the scheme, protected from electrically induced signals with mesh shields *4* and *6*. The assembly comprised of the target and all analyzer electrodes can be displaced in two transverse directions, thus allowing scanning of the input aperture over the beam cross-section.

For realization of electric cut-off method, application of a large electric potential is necessary, which makes electric strength the key problem, especially in the presence of the dense high-power beam. Special configuration of electrodes was designed to reduce energy loads at electrode surfaces and to suppress the discharge phenomena. The input aperture 1 mm in diameter not only allows to measure parameters of the beam at a local position, but also serves to reduce current density − due to transverse velocities of electrons, the

beam cross-section substantially expands in the analyzer soon after the pin-hole. Mesh electrodes are placed in the areas with weak electric field to avoid problems with expansion of plasma and secondary particle flows as well as mesh sparking in strong pulsed fields. High-voltage gaps are 20 − 30 mm wide. Near the system axis, where the most part of the studied beam propagates, the electric potential varies with approximately constant rate over ~12 cm length (Fig. 2), thus peak electric field strength is minimized. To reduce secondary emission effects, all apertures have conical shapes with sharp edges.

Besides the axial energy distribution measured during a single facility pulse, the new analyzer may be used to define the transverse component of electron energy, even though it requires a series of shots. The special data-processing techniques are discussed in the next chapter. To implement this function, the analyzer is equipped with built-in coils for magnetic field distribution control in the
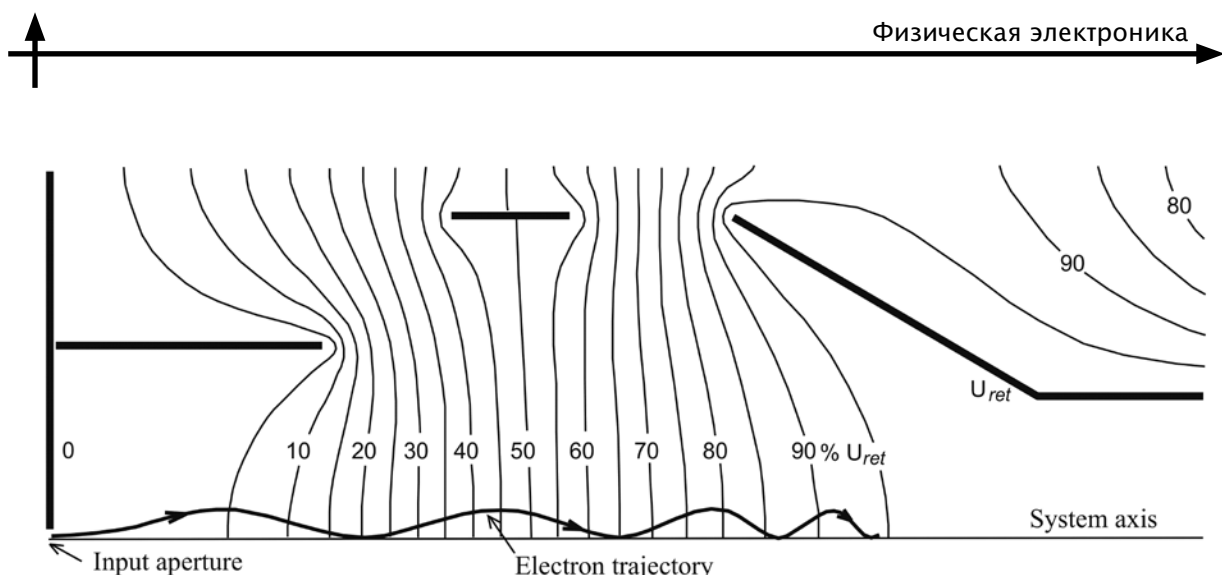
Fig. 2. Distribution of the electric potential in the analyzer (in % of the U_{ret} value) and a typical electron trajectory in the uniform magnetic field ($B_0 = 0.1$ T, $W = 60$ keV, pitch angle is 15°)

analyzer volume (see $B(z)$ plots in Fig. 1). This field does not penetrate upstream from the target, thus disturbance of either the whole facility beam or target conditions is practically excluded.

3. Data processing: approach and technique

Soffron60 measurement data (Fig. 3a) have initial form of 5 oscillograms: 2 voltage pulses (facility gun cathode potential U_0 and the voltage applied to the retarding electrode U_{ret}) and 3 analyzer collector currents (I_{in}, I_{pass} and I_{refl}, see Fig. 1). In the absence of discharges and other parasitic phenomena, we can expect these current waveforms to be in agreement:

$$I_{in}(t) = a_1 I_{pass}(t) + a_2 I_{refl}(t), \qquad (1)$$

where constants a_1 and a_2 account for nonequivalent collector properties, such as geometric areas, grid transparencies, etc.

Considered jointly with the potentials waveforms, the collector currents may be used to calculate normalized integral energy distribution (also known as "cut-off function") $S(u)$ defined as relative number of electrons having axial energy $W_\parallel$ sufficient to get over the retarding electric potential characterized by normalized value

$$u(t) = U_{ret}(t) / U_0(t).$$

A derivative of a cut-off curve gives us the electron axial energy distribution in the input beam: $N(W_\parallel) = - dS/du$.

According to Eq.(1), there are three ways

to calculate the cut-off function from the experimental data:

$$S_1(u(t)) = a_1 I_{pass}(t) / I_{in}(t), \qquad (2a)$$

$$S_2(u(t)) = 1 - a_2 I_{refl}(t) / I_{in}(t), \qquad (2b)$$

$$S_3(u(t)) = a_1 I_{pass}(t)[a_1 I_{pass}(t) + a_2 I_{refl}(t)]^{-1}. \qquad (2c)$$

If the analyzer operates properly, these three functions must coincide (Fig. 3b). Their substantial divergence would show that the input beam is not the only significant current source in the analyzer, and the registered data should be discarded as dubious.

The cut-off curves $S(u)$ measured with uniform magnetic field distribution in the analysis volume (conserving transverse energy component $W_\perp$) represent axial energy distribution $N(W_\parallel)$ at the target. When the built-in analyzer coils are turned on to make the magnetic profile nonuniform, the energy redistributes between the components while the beam moves from the target to the retarding space, which affects the investigated $N(W_\parallel)$ spectra. The magnetic profile distortion degree can be characterized with "magnetization" parameter $\beta = B_a / B_0$, where B_0 and B_a are magnetic induction values for the target plane and a position of the retarding potential minimum (see plot in Fig. 1) respectively. A set of spectra measured for the same beam parameters and different β can yield information on full 2D energy distributions $N(W_\parallel, W_\perp)$.

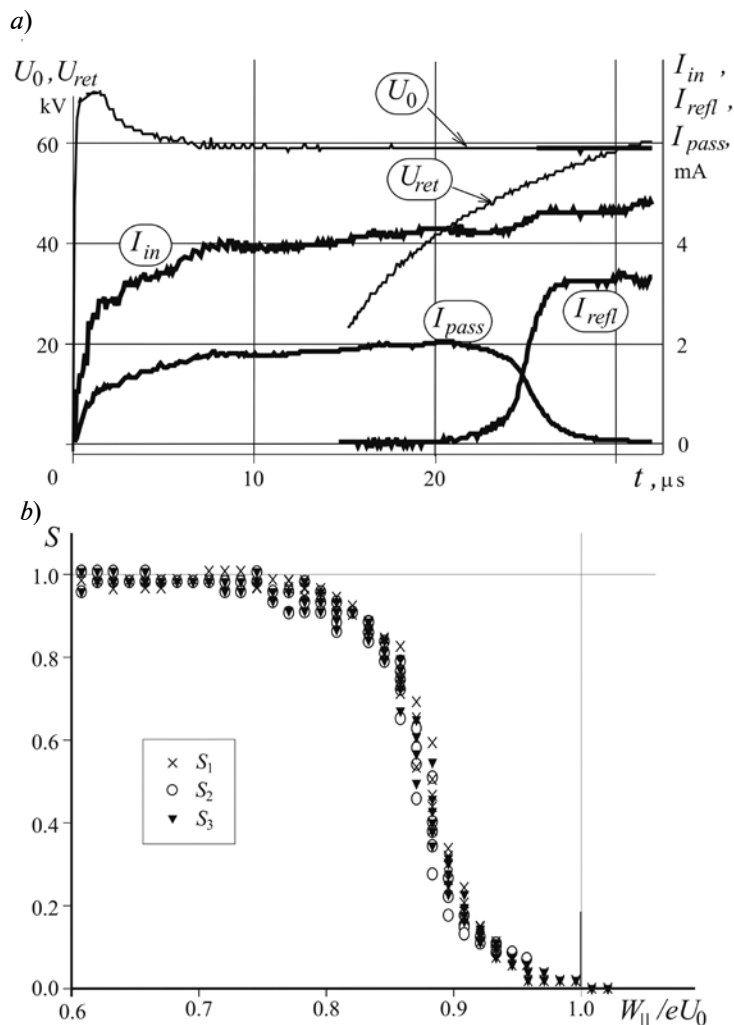The law of the energy exchange between the components is the simplest for "adiabatic"

a)

b)

Fig. 3. A typical set of oscillograms acquired in the Soffron60 test experiments, including accelerating and retarding potentials (U_0, U_{ret}) and currents to three current probes (*a*); integral spectrum *S* of axial electron energy corresponding to these data (*b*). S_1, S_2, S_3 were calculated in accordance with different definitions given by formulae (2a), (2b), (2c), respectively

conditions, when variation of magnetic and electric fields in space is slow:

$$\begin{cases} \left| d(B, E) / (B, E)dr \right| \ll 1 / R_L; \\ \left| d(B, E) / (B, E)dz \right| \ll 1 / L_L, \end{cases} \quad (3)$$

where R_L and L_L are Larmor parameters of electron trajectory;

$$R_L = (2W_\perp / m)^{1/2} / \omega_L;$$

$$L_L = 2\pi(2W_\parallel / m)^{1/2} / \omega_L;$$

$\omega_L = eB/m$ is Larmor cyclic frequency; *e* and *m* are electron charge and mass.

In adiabatic case, the transverse energy of any electron is proportional to the magnetic field at its current position *B*, while its full energy *W* remains constant:

$$W_\perp = (B/B_0)\ W_{\perp 0}; \quad (4a)$$

$$W_\parallel = W - W_\perp = W_{\parallel 0} + W_{\perp 0} - W_\perp = \\ = W_{\parallel 0} - W_{\perp 0}\ (B/B_0 - 1). \quad (4b)$$

Index 0 marks the values corresponding to a fixed initial axial position of the particle that we choose coinciding with the input aperture of the analyzer and with the target plane, where

the magnetic field B_0 is the same for all shots of a series.

In theory, axial energy spectrum $N(W_\parallel)$ obtained by derivation of a cut-off curve may be considered also as a result of convolution (integration, projection) of two-dimensional distribution at the spatial position of measurement $N(W_\parallel, W_\perp)$ along vertical lines $W_\parallel = $ const. In the case of uniform magnetic field, no energy transform between components occurs, and such connection can be established between the measured spectra $N(W_\parallel)$ and the 2D energy distribution at the target $N(W_{\parallel 0}, W_{\perp 0})$ characterizing the investigated facility flow (see Fig. 4a). When the field in the analyzer is made nonuniform, the axial energy spectrum $N(W_\parallel)$ is vertical projection of 2D energy distribution in the point of measurement $N(W_\parallel, W_\perp)$ (Fig. 4b), transformed according to formulae (4). At the target position, the field does not change, and the energy distribution in $(W_{\parallel 0}, W_{\perp 0})$ coordinates is the same as that in the uniform field (Fig. 4c).

Approached formally, relations (4) can be interpreted as description of a linear transformation of the coordinate plane $(W_{\parallel 0}, W_{\perp 0}) \to (W_\parallel, W_\perp)$ with β serving as a parameter. This transformation reflects any straight line of

$(W_\parallel, W_\perp)$ onto another straight line crossing the abscissa axis at the same point and having β times greater (for β > 1) angle to positive direction of the abscissa axis (see Fig. 5). The image line will be vertical ($\alpha' = \pi/2$), if the angle of the initial line slope is equal to

$$\alpha = \mathrm{arctg}(\beta - 1)^{-1}. \qquad (5)$$

Thus, returning to Fig. 4b, c, we can use the fact that integration (projection, convolution) along vertical projection lines at the $(W_\parallel, W_\perp)$ plane is equivalent to the integration along straight lines sloped by α in $(W_{\parallel 0}, W_{\perp 0})$ coordinates. Consequently, the axial energy distributions measured for different values of β parameter (they will be denoted as $N_\beta(W_\parallel)$) can be considered as parallel projections of 2D energy distribution at the target $N(W_{\parallel 0}, W_{\perp 0})$ under different aspect angles α determined by Eq. (5). In practice, rather broad range of aspect angles may be available: α is small in the case of high magnetization in the analyzer (for instance, $\alpha = \pi/4$ for β = 2), and is close to $3\pi/4$ if the built-in coils substantially reduce the external guiding magnetic field (β → 0).

The problem of reconstruction of a full 2D function from a set of projections is known as "tomography problem", and has been
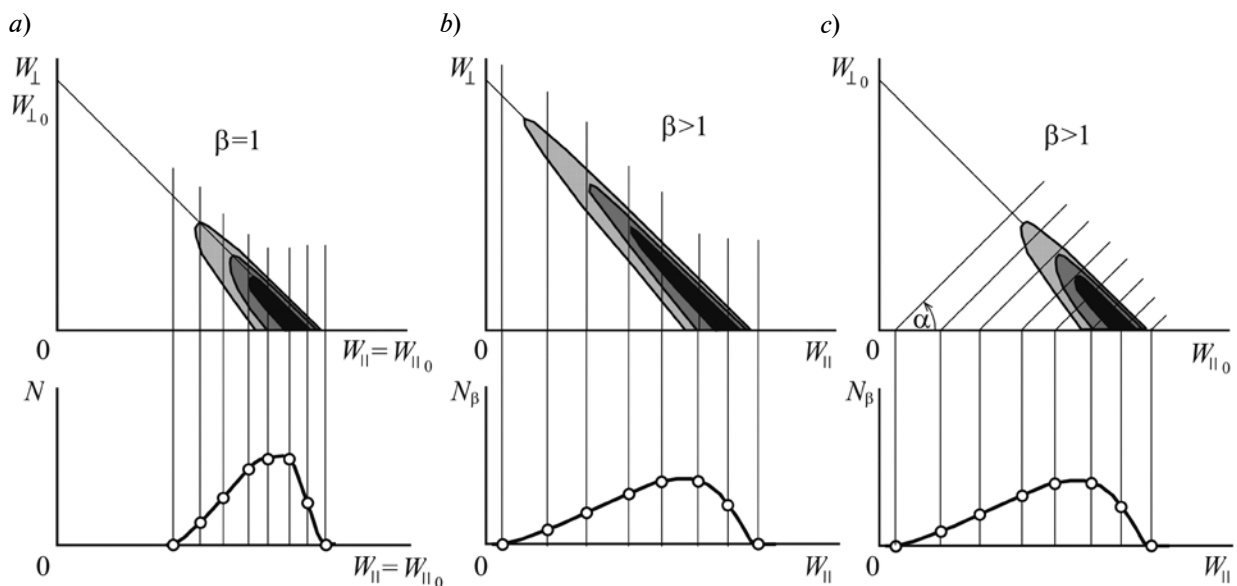

Fig. 4. Reconstruction of 2D electron energy distributions.
Axial energy spectrum is measured: (a) in uniform magnetic field (β = 1); (b), (c) − in increasing magnetic field (β > 1). This spectrum may be represented in two ways: (b) as the vertical projection of 2D energy distribution at the position of measurement or (c) as the projection of 2D energy at the target under the aspect angle $\alpha = \mathrm{arctg}(\beta - 1)^{-1}$
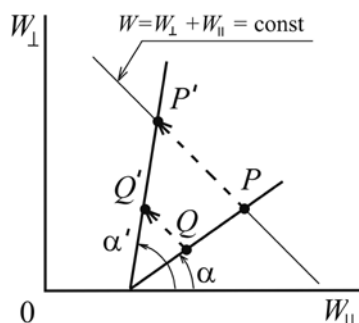
Fig. 5. Transformation of $(W_{\parallel}, W_{\perp})$ plane described by formulae (4) (adiabatic case).
Any given point P is reflected onto a point P' belonging to the same straight line W=const. Any straight line PQ is reflected onto the straight line $P'Q'$ crossing the abscissa axis at the same point. The angle of inclination to the axis is multiplied by β

extensively studied for medicine and plasma physics applications, and the corresponding mathematical methods could be used in our case. Though, a specific feature of the data acquired in experiments with intense high-energy electron beams consists usually in rather large shot-to-shot scatter of measured characteristics that would require simpler and more direct data processing technique. For instance, instead of 2D distribution, we might choose to acquire full electron energy spectrum $N(W)$ that can be determined as the limit of $N_{\beta}(W_{\parallel})$ for $\beta \rightarrow 0$.

For the above speculations, adiabatic character of electron motion in the area of analysis was assumed. In principle, such assumption is not strictly necessary. If the conditions of experiment do not satisfy to relations (3), electron energy transfer in the system would be nonlinear, and the corresponding convolution (projection) lines at the $N(W_{\parallel}, W_{\perp})$ plane are not straight lines but curves. Still, the problem of deconvolution of a set of measured axial energy spectra $N_{\beta}(W_{\parallel})$ may be solved if we know precise shape of these lines. Such information can be obtained, for instance, by digital simulation of electron trajectories in the analyzer fields, and it allows determining cut-off potentials for different parameters of test particles.

4. Instrumental errors

The following factors were expected to contribute most substantially in the instrumental error of energy analysis and to determine its resolution:

(a) non-ideal distribution of the retarding electric field;

(b) energy redistribution between velocity components due to non-adiabatic character of electron motion in the analyzer;

(c) nonuniform electric fields at the input aperture;

(d) space-charge electric field in the analyzer;

4.1. Non-ideal EOS properties

In the ideal electron-optical system (EOS) for analysis of axial component of electron energy, the retarding electric field equipotential surfaces must be flat and parallel within the volume occupied by the studied beam. To achieve such structure, use of fine-mesh electrodes would be most natural. Though, very probable problems with electric strength and secondary particles originating at meshes in strong electric field under electron bombardment made this solution objectionable. In Soffron60 analyzer, the retarding field is formed with a system of large-diameter cylindrical and conical electrodes optimized to produce maximally flat equipotentials near the axis, where the most part of the investigated beam propagates (see Fig. 2). At the same time, the radial electric field component away off the axis is non-zero and grows with radius, affecting electron motion on trajectories with large transverse oscillation amplitudes. Another source of instrumental error can be connected with a difference between the negative potential applied to the retarding electrode and the minimum potential values at electron trajectories. In a system of limited axial length, this difference is nonzero. Both these effects were evaluated quantitatively by numeric simulation of single-electron trajectories in the EOS fields. Values of the retarding potential sufficient to reflect electrons with different injection parameters were determined. Simultaneously, effects of nonadiabatic electron energy transformation between axial and transverse components in nonuniform fields were estimated for different values of B_0. The overview of the simulation results is presented in Fig. 6. For full electron energy $W = 60$ keV, the guiding

magnetic field $B_0 = 0.1$ T was found to secure accurate performance of the analyzer (Fig. 6*a*): disagreement of the cut-off potential values with ideal "adiabatic" predictions does not exceed 0.5% *W*. For lower magnetic field $B_0 = 0.04$ T and $W = 60$ keV, electron Larmor step $L_L \approx 13$ cm is comparable with the analyzer length, which results in much larger disagreement (Fig. 6*b*). For uniform magnetic field ($\beta = 1$), the axial energy measurement error grows up to 2 %*W*, and is even much worse for high magnetization ratios. In this case, corresponding corrections must be introduced in the data processing routine.

4.2. Effect of the electron space charge fields

Accurate calculation of electron space charge contribution $\Delta\Phi$ in electric potential in the analyzer represents a self-consequent and therefore complicated problem. Though, rough upper estimate of its value can be obtained using the formula for a uniform solid cylindrical (radius r_b) beam with full current I_b in a long conductive tube (radius r_a):

$$|\Delta\Phi| = I_b(1/2 + \ln(r_a/r_b))/2\pi\varepsilon_0 v_\parallel, \quad (6)$$

where $v_\parallel = (2W_\parallel/m)^{1/2}$ is an axial velocity of electrons.

The current of the partial beam cut with 1 mm input aperture I_b for the maximum design current density of 10 A/cm² is approximately 80 mA. Inner radius of the analyzer electrodes is no larger than $r_a = 50$ mm. Radius of the beam r_b in the analysis area can be estimated
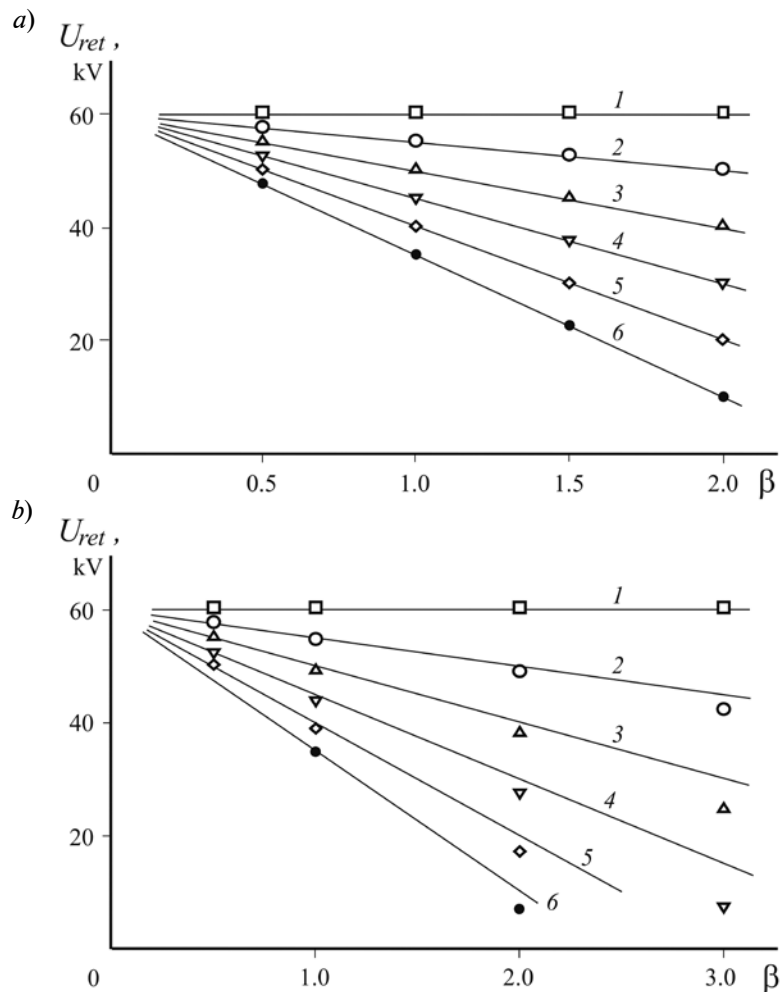

Fig. 6. Reflecting values of retarding potential vs magnetization ratio for electrons with full energy $W = 60$ keV at the different transverse energies $W_\perp$, calculated by trajectory simulations for two target magnetic field strengths: $B_0 = 0.10$ T (*a*) and 0.04 T(*b*). $W_\perp$, keV: 0 (line *1*), 5 (*2*), 10 (*3*), 15 (*4*), 20 (*5*), 25 (*6*)

by Larmor diameter of a typical electron trajectory (see Fig. 2) as approximately equal to 5 mm for $W = 60$ keV, $B_0 = 0.1$ T and the pitch angle 15°[2]. According to Eq. (6), these values give us $|\Delta\Phi| \approx 30$ V or 0.05% W/e, if no retarding potential is applied to the analyzing electrodes. If the retarding potential is applied and all electrons are decelerated to $W_{\parallel} = 0.01$ W (the beam is now assumed to be ideally monoenergetic), the space-charge potential will grow to 0.5% W/e, which is also quite acceptable. Further deceleration should not be considered with the long-tube formula (6), because axial length of the region were it might be realized would be shot compared to any possible radial dimensions. Thus, maximum space-charge potential contribution to the instrumental error can be evaluated as 0.5 %.

4.3. Electric field at the input aperture

Another possible error source originates in strong nonuniformity of electric field introduced by the input pin-hole aperture. On their way through nonuniform static field, electrons do not change full energy. Though, the energy can be redistributed between axial and transverse components due to nonadiabatic character of motion inside and near the small-size (radius $r_0 = 0.5$ mm) aperture. In the developed EOS design, the electric field strength at the back (analyzer) side of the target is rather week − less than 1 kV/cm even for the highest retarding potentials. Space-charge fields in high-current facility beam are much stronger − up to $E_t \approx 10$ kV/cm − at least, during first microseconds of a pulse, while effects of target plasma and/or ion accumulation are not fully developed. Upper estimate of the additional transverse velocity acquired by an electron with initial velocity components $v_{\parallel}$ and $v_{\perp}$ on its way through the nonadiabatic field-distortion area can be given as

$$\delta v_{\perp} \approx eE_t r_0/m_e v_{\parallel}.$$

The corresponding contribution to the transverse energy is as follows:

$$\delta W_{\perp} \approx m_e v_{\perp} \delta v_{\perp} \approx eE_t r_0 v_{\perp}/v_{\parallel}. \qquad (7)$$

For typical value $v_{\perp}/v_{\parallel} = 0.3$, this gives us an error in energy component measurement $\delta W_{\perp} \approx 300$ eV = 0.5 % W.

4.4. All-over instrumental error and energy resolution

The above considerations allow estimating energy resolution of Soffron60 apparatus as being not far from 1 %. This quantity does not include possible contributions from manufacture and assembly imperfection, errors of electronic instrumentation, etc. Also, there are a number of factors (one of them is different transparency of grids and apertures for partial flows with different trajectory parameters) that do not change energy of electrons but can affect relative heights of peaks in measured energy distributions. Some other parasitic phenomena, including secondary emission from complex electrodes, cannot be given adequate quantitative account. Their possible role was estimated in experimental tests of the new apparatus performed prior to its full-scale use at one of GESA facilities.

5. The experimental test of the analyzer

The test experiments were performed at EPVP experimental stand at St. Petersburg Polytechnic University [3, 4]. Characteristic feature of this installation is very high beam compression ratio (up to 1 500) allowing to achieve high energy density at the target using the beam produced by thermionic-cathode gun with rather modest current of $0.2 - 4.0$ A. For these tests, the stand was reconfigured to comply with the task requirements: electron energy $eU_0 \leq 60$ keV, current density at the target $0.1-10$ A/cm^2, guiding magnetic field $0.05-0.20$ T, pulse length $20-100$ μs.

Fig. 3 presents a typical set of experimental waveforms including full current I_b and acceleration voltage U_0 of the EPVP beam, retarding voltage pulse U_{ret} and currents onto three collectors of the analyzer. As expected, when U_{ret} value approached U_0, the current of reflected particles I_{refl} grew in accordance with reduction of passing-through current I_{pass}. Calculation of cut-off curves from three couples of currents using formulae (2a) − (2c) gives coinciding results (see Fig. 3b), thus confirming validity of the data.

Cut-off curves (or integral axial energy distributions) measured in different conditions
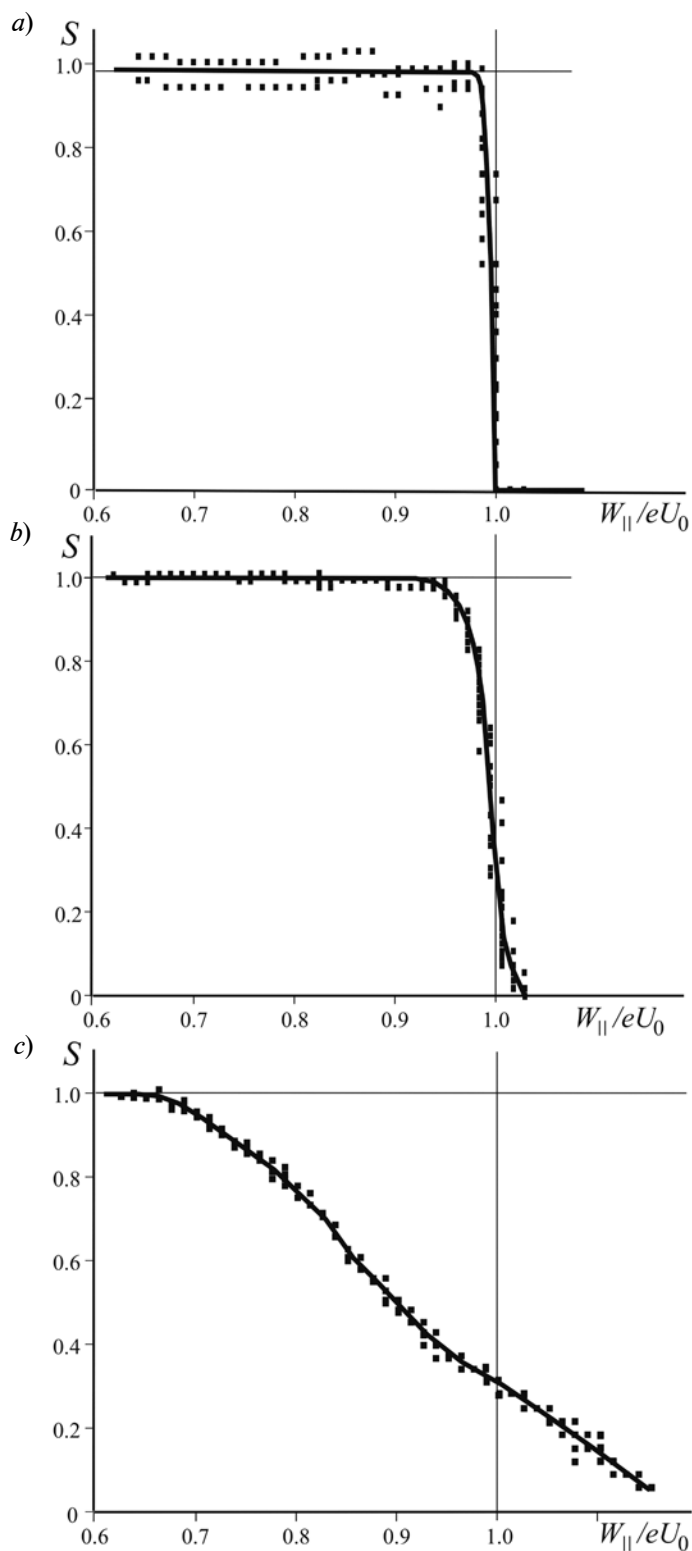
Fig. 7. Narrow (*a*, *b*) and broad (*c*) integrated spectra of axial energy $S(W_\parallel)$ measured for the electron beam of EPVP stand under different regimes (gun voltage, magnetic induction of uniform field, beam current): 30 kV, 0.075 T, 0.15 A/cm² (*a*); 60 kV, 0.125 T, 0.4 A/cm² (*b*); 60 kV, 0.125 T, 0.1 A/cm²) (*c*)
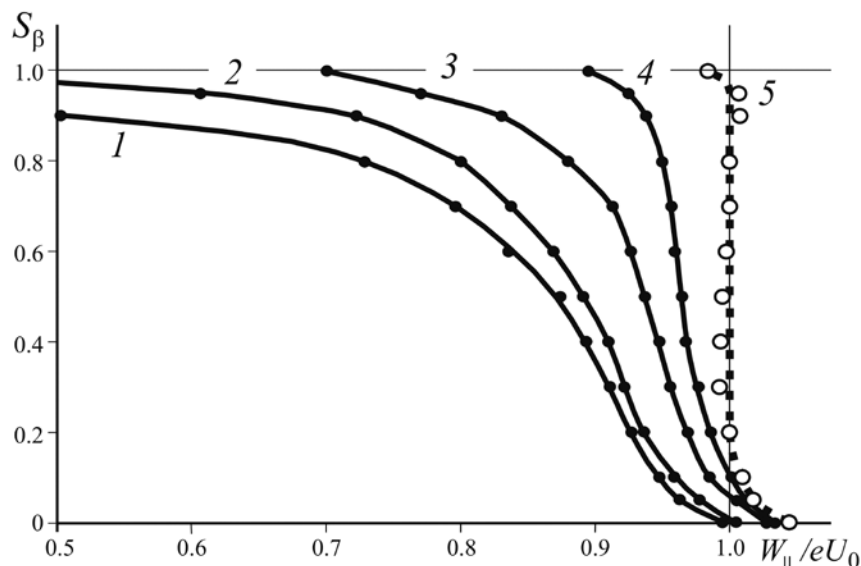
117

Fig. 8. A few typical integrated spectra S_β ($W_\parallel$) measured for different β parameter values: 2.54 (*1*), 1.75 (*2*), 0.96 (*3*), 0.38 (*4*), 0 (*5*, extrapolation to 0); a regime without notable beam energy losses or rf oscillations

were substantially different. Spectra for the central part of the beam (see Fig. 7*a*, *b*) were substantially narrower than those for the periphery (Fig. 3*b*), which is natural for the beam compression scheme used at the EPVP [3]. The minimum width of the spectrum registered in those tests was as low as about $1.5 - 2.0$ % (Fig. 7*a*). This figure gives an upper limit of axial energy resolution provided by the analyzer: most probably, the resolution is better, because the test beam spectrum width is not likely to be exactly zero even in "the best" shot. In some cases, broad energy distributions were observed, with large number of abnormally accelerated particles with $W_\parallel$ up to 1.2 eU_0 (Fig. 7*c*). Such spectra are explained by development of radiofrequency oscillations scattering the beam in space and energies, which previously were often observed in EPVP beam in similar conditions.

Axial energy spectra $N_\beta(W_\parallel)$ measured with different analyzer magnetization for the same EPVP regime demonstrated monotonous transformation with variation of β. In the absence of radiofrequency oscillations, the measured spectra were narrowest (Fig. 8), and their extrapolation to β = 0 gave us the full-energy distribution $N(W)$ of practically zero width (dashed line). This confirms feasibility of

the proposed method of determination of the second energy component.

Thus, the tests have demonstrated correct operation of the analyzer in the conditions of experiment. Comparatively easy achievement of this goal shows that this scheme or even this apparatus can be successfully used with beams having higher energies (at least, up to 100 keV, and, maybe, more).

6. Summary

The newly developed analyzer Soffron60 is designed for operation with GESA electron-beam material-treatment facilities [1] and can be used at machines with similar characteristics (~60 kV, ~100 A, ~100 µs, 0.1 T) or even with more energetic beam. The analyzer allows determination of electron energy distributions with resolution in space and time (1 mm, 10 µs). For axial energy spectrum measurement, electric cut-off scheme is realized. Information on distributions of transverse or full energy can be derived from cut-off curves measured in the presence of additional magnetic field in the analysis area. Energy resolution of the developed diagnostic system is ~1 %. Test experiments have demonstrated proper operation of the apparatus and good agreement of its observed parameters with expectations.

REFERENCES

[1] **V. Engelko, B. Yatsenko, G. Mueller, H. Bluhm,** Pulsed electron beam facility (GESA) for surface treatment of materials, Vacuum. 62 (2) (2001) 211—216.

[2] **V. Engelko, G. Mueller, V. Kovalev, O. Komarov,** Measurement of angular distribution of beam electrons at GESA facilities, BEAMS 2002: 14th International Conference on High-Power Particle Beams, in: AIP Conf. Proc. 650 (1) (2002) 329—332.

[3] **A.V. Arkhipov, G.G. Sominski,** Vacuum insulation and discharge phenomena in high-power devices with magnetic confinement of electron flow, IEEE Transactions on Dielectrics and Electrical Insulation. 6 (4) (1999) 491—500.

[4] **A.V. Arkhipov, G.G. Sominski,** Interaction of a long pulsed high-density electron beam with a jet of solid-target destruction products, Technical Physics. 46 (9) (2001) 1106—1111.

THE AUTHORS

ARKHIPOV Alexander V.
St. Petersburg Polytechnic University
29 Politekhnicheskaya St., St. Petersburg, 195251, Russian Federation
arkhipov@rphf.spbstu.ru

MISHIN Maxim V.
St. Petersburg Polytechnic University
29 Politekhnicheskaya St., St. Petersburg, 195251, Russian Federation

SOMINSKI Gennadi G.
St. Petersburg Polytechnic University
29 Politekhnicheskaya St., St. Petersburg, 195251, Russian Federation
sominski@rphf.ru

А.В. Архипов, М.В. Мишин, Г.Г. Соминский. АНАЛИЗАТОР ДЛЯ СИЛЬНОТОЧНЫХ ЭЛЕКТРОННЫХ ПУЧКОВ С РАЗРЕШЕНИЕМ ПО ДВУМ СОСТАВЛЯЮЩИМ ЭНЕРГИИ, ПОЛОЖЕНИЮ И ВРЕМЕНИ.

Разработано устройство для экспериментальной регистрации энергетических и пространственных распределений плотных электронных пучков умеренных энергий, транспортируемых в магнитном поле — с типичными параметрами 10 А/см², 60 кэВ, 100 мкс, 0,1 Тл. Использование метода тормозящего электрического поля позволяет получить детальную, прямую и непротиворечивую информацию об энергетических спектрах электронов. В сочетании с меняющимся магнитным полем в области энергоанализа, метод позволяет раздельно определять аксиальную и поперечную составляющие энергий электронов. Экспериментальное тестирование подтвердило, что энергетическое разрешение анализатора составляет ~1%, как и предсказывалось расчетами, учитывающими неидеальность форм электродов, влияние пространственного заряда и отклонение от адиабатичности условий преобразования энергии в меняющемся магнитном поле. Пространственное и временное разрешение анализатора определяются соответственно размером входной апертуры (~1 мм) и длительностью импульса задерживающего поля (5 —10 мкс).

ЭЛЕКТРОНЫЙ ПУЧОК, ЭНЕРГЕТИЧЕСКОЕ РАСПРЕДЕЛЕНИЕ ЭЛЕКТРОНОВ, АНАЛИЗАТОР С ТОРМОЗЯЩИМ ПОЛЕМ, ЭЛЕКТРОННО-ОПТИЧЕСКАЯ СИСТЕМА.

СПИСОК ЛИТЕРАТУРЫ

[1] **Engelko V., Yatsenko B., Mueller G., Bluhm H.** Pulsed electron beam facility (GESA) for surface treatment of materials // Vacuum. 2001. Vol. 62. No. 2. Pp. 211—216.

[2] **Engelko V., Mueller G., Kovalev V., Komarov O.** Measurement of angular distribution of beam electrons at GESA facilities // BEAMS 2002: 14th International Conference on High-Power Particle Beams, in: AIP Conf. Proc. 2002. Vol. 650. No. 1. Pp. 329—332.

[3] **Arkhipov A.V., Sominski G.G.** Vacuum insulation and discharge phenomena in high-power devices with magnetic confinement of electron flow // IEEE Transactions on Dielectrics

and Electrical Insulation. 1999. Vol. 6 No. 4. Pp. 491−500.

[4] **Arkhipov A.V., Sominski G.G.** Interaction of a long pulsed high-density electron beam with a jet of solid-target destruction products // Technical Physics. 2001. Vol. 46. No. 9. Pp. 1106−1111.

СВЕДЕНИЯ ОБ АВТОРАХ

АРХИПОВ Александр Викторович − *кандидат физико-математических наук, доцент кафедры физической электроники Санкт-Петербургского государственного политехнического университета.*
195251, Российская Федерация, г. Санкт-Петербург, Политехническая ул., 29
arkhipov@rphf.spbstu.ru

МИШИН Максим Валерьевич − *кандидат физико-математических наук, докторант кафедры «Физико-химия и технологии микросистемной техники» Санкт-Петербургского государственного политехнического университета.*
195251, Российская Федерация, г. Санкт-Петербург, Политехническая ул., 29
maximvmishin@gmail.com

СОМИНСКИЙ Геннадий Гиршевич − *доктор физико-математических наук, профессор кафедры физической электроники Санкт-Петербургского государственного политехнического университета.*
195251, Российская Федерация, г. Санкт-Петербург, Политехническая ул., 29
sominski@rphf.spbstu.ru